

The Interaction of Extended Defects as the Origin of Step Bunching in Epitaxial III–V Layers on Vicinal Si(001) Substrates


Michael Niehle,* Jean-Baptiste Rodriguez, Laurent Cerutti, Eric Tournié, and Achim Trampert

Several nanometer high steps are observed by (scanning) transmission electron microscopy at the surface and interfaces in heteroepitaxially grown III–Sb layers on vicinal Si(001) substrates. Their relations with antiphase boundaries (APBs) and threading dislocations (TDs) are elaborated. An asymmetric number density of TDs on symmetry-equivalent {111} lattice planes is revealed and explained according to the substrate miscut and the lattice misfit in the heteroepitaxial material system. Finally, a step bunching mechanism is proposed based on the interplay of APBs, TDs, and the vicinal surface of the miscut substrate.

Step bunching is a well-established term in the field of layer-by-layer (2D) homo- or heteroepitaxial crystal growth.^[1] An angular deviation from a low-indexed surface of the crystalline growth substrate (vicinal surface/miscut substrate) leads to the presence of terraces separated by steps from one to several atomic monolayer heights. Adatoms diffuse on the terraces during growth until they meet an ascending or descending step. Depending on the potential barrier at the step—the Ehrlich-Schwoebel barrier^[2]—adatoms may anisotropically stick, leading to step bunching and an increase in terrace widths in case of the descending step.^[3] Nevertheless, terrace widths are limited by diffusion length because 2D nucleation finally sets in on the terraces.^[1]

Dr. M. Niehle, Dr. A. Trampert
Microstructure Department
Paul-Drude-Institut für Festkörperphysik
Hausvogteiplatz 5-7, 10117 Berlin, Germany
E-mail: niehle@pdi-berlin.de

Dr. J.-B. Rodriguez, Dr. L. Cerutti, Prof. E. Tournié
Institut d'Electronique et des Systèmes (IES)
Université Montpellier – CNRS, UMR 5214
Montpellier F-34000, France

 The ORCID identification number(s) for the author(s) of this article can be found under <https://doi.org/10.1002/pssr.201900290>.

© 2019 The Authors. Published by WILEY-VCH Verlag GmbH & Co. KGaA, Weinheim. This is an open access article under the terms of the Creative Commons Attribution-NonCommercial-NoDerivs License, which permits use and distribution in any medium, provided the original work is properly cited, the use is non-commercial and no modifications or adaptations are made.

The copyright line for this article was changed on 18 November 2019 after original online publication.

DOI: 10.1002/pssr.201900290

In this work, a different mechanism of step bunching is described. It is based on observations by scanning transmission electron microscopy (STEM) and electron tomography. First, several nanometer high-surface and interface steps are shown to coincide with antiphase boundaries (APBs). Subsequently, an imbalance in the number of threading dislocations (TDs) on the different glide systems is outlined. Reference is made to the trapping of TDs by APBs demonstrated by electron tomography in a recent work.^[4] Eventually, the step

bunching mechanism is deduced from the interaction of these extended defects and the application of a miscut substrate.

Antimonide-based infrared laser structures fabricated on Si(001) substrates are considered in this work. This heterostructure is paradigmatic for the heteroepitaxial growth of polar III–V compound semiconductors with zinc blende structures on nonpolar substrates with diamond structures (Si, Ge). The integration of both material classes promises to exploit the opto-/electronic properties of III–V materials while retaining the economic and technologically mature substrates. Respective material systems find manifold opto-/electronic applications, e.g., as transistors, solar cells, and light emitting diodes. The investigated material system consists of III–Sb layers (group III elements: Al, Ga, In) epitaxially grown on Si(001) substrates by molecular beam epitaxy (MBE). Besides nominal on-axis Si(001) wafers, vicinal Si(001) substrates are used, exhibiting miscut angles of 3° and 7° tilting of the surface normal to the [110] direction. The miscut substrates are usually applied for the presented laser structures^[5,6] to suppress the formation of APBs. These defects are known to deteriorate electronic properties.^[7] The miscut allows for the formation of atomic double steps and, consequently, a single-domain surface reconstruction.^[8] On the other hand, there are endeavors to suppress APB formation on nominal Si(001) wafers because they present the established industrial standard.^[9] The sequence of III–Sb layers is depicted in **Figure 1**. An AlSb wetting layer (not indicated) has been deposited onto the substrate prior to the growth of the initial GaSb buffer layer. The subsequent layers form an infrared laser structure with the In-rich quantum wells in the center of the stack. MBE growth details of a similar sample can be found in studies by Rodriguez et al.^[5]

Cross-sectional and plan-view specimens have been prepared by focused ion-beam sample preparation, applying the lift-out technique, except for one specimen that has been prepared

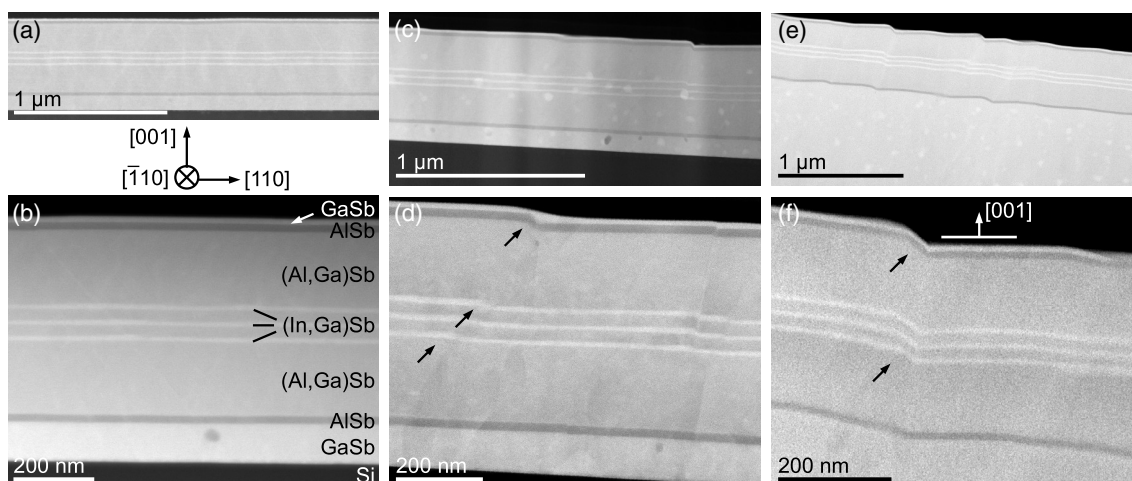


Figure 1. HAADF STEM images of cross-sectional specimens are presented. The columns refer to samples grown on nominal and 3° and 7° miscut Si(001) substrates, respectively. Upper images show an overview and lower ones a magnified part around the surface and interface steps. (Black arrows indicate steps at heterointerfaces.).

by mechanical thinning and final Ar-ion polishing. The latter one has been used for convergent beam electron diffraction (CBED) measurements. Transmission electron microscopy (TEM) and STEM measurements have been carried out using a JEOL 2100F electron microscope.

Figure 1 displays STEM images of three cross-sectional specimens prepared from three different samples. The images of the first column represent the heterostructure grown on the nominal on-axis Si(001) substrate. The images of the second and third one belong to the cases of 3° and 7° miscut substrates, respectively. The micrographs are acquired in the high-angle annular dark-field (HAADF) STEM mode. This imaging mode is sensitive to the atomic number (Z-contrast) of the layer material. The atom density in the III–Sb layers is regarded as constant. All images present the views along the [110] zone axes which correspond to the prevailing surface step direction of the miscut substrates. In the images, the [001] direction is chosen to be vertical instead of surface normals in order to underline the substrate miscut angles. The growth on nominal Si(001) appears to result in smooth surfaces as shown in Figure 1a,b. In contrast, an increasing surface roughness is observed in samples grown on vicinal surfaces with increasing miscut angles as observed in Figure 1c,e. Figure 1d,f are magnified parts of the epitaxial layer, emphasizing the presence of several nanometer high steps at the surface and at the heterostructure interfaces (black arrows). The view along the perpendicular [110] direction which is not parallel to the interface of the miscut substrate usually reveals “blurred” layers (not shown here). Nevertheless, sharp interfaces are sometimes observed due to the occasional presence of well-shaped (001) terraces at the bottom of a step as outlined in Figure 1f.

An extended planar defect is always observed accompanying the described steps. **Figure 2a** shows a bright-field (BF) TEM image, reflecting steps in the AlSb and the (In,Ga)Sb layers and the presence of an extended defect. A series of CBED patterns has been acquired along the arrow. Colored dots allow the allocation of CBED data presented in Figure 2b. Passing

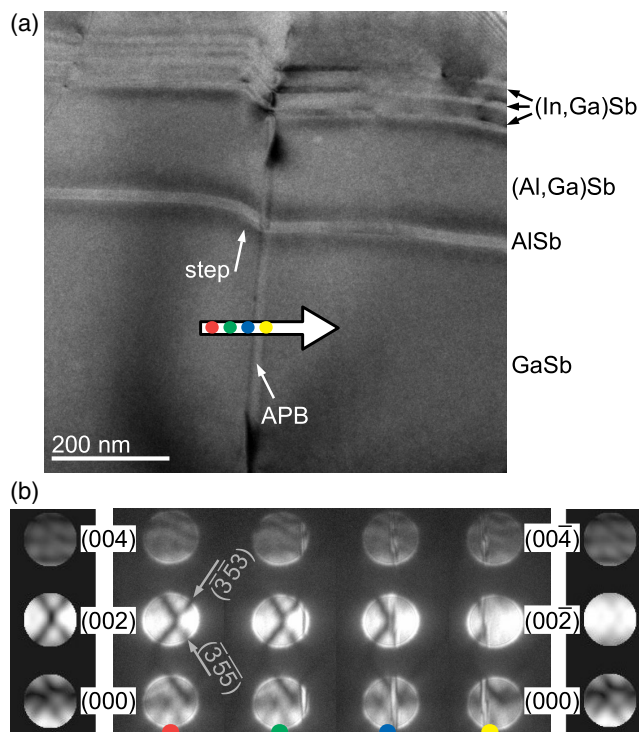


Figure 2. a) A bright-field TEM image depicts the presence of a step and the sites of CBED acquisitions across a planar fault viewed nearly edge on. b) The scan of CBED patterns is shown along with calculated patterns.

the fault with the converged beam leads to the change in the dark cross through the (002) reflection. This dark feature arises due to the destructive interference of the odd-numbered Kikuchi lines (belonging, here, to the $(\bar{3}\bar{5}3)$ and the $(\bar{3}\bar{5}\bar{5})$ lattice planes) with the (002) reflection. The change arises because there is the (002) reflection on the right-hand side of the planar defect, interfering

constructively with the Kikuchi lines.^[10] Consequently, the extended defect is ascribed to an APB.

The cross-sectional BF STEM overview image in **Figure 3a** unveils a larger number of TDs on $(\bar{1}\bar{1}1)$ than on (111) lattice planes in the sample grown on the 7° miscut substrate. The selected area diffraction (SAD) pattern shown in **Figure 3b** shows pairs of diffraction spots belonging to the substrate (a larger distance to the central beam) and the epitaxial GaSb buffer layer. It underlines the epitaxial relation of the Si and the III–Sb lattices. There is not a measurable lattice tilt between the substrate and epitaxial layers due to the asymmetry in the distribution of extended line defects on a scale of micrometers.

For the following discussion, the presented experimental observations are complemented with electron tomography results from a recent publication.^[4] The tomographic analysis has highlighted the interaction of TDs with APBs which is depicted in the scheme of **Figure 4b**. TDs tend to bend into APBs (red arrow) instead of

residing on their usual $\{111\}$ glide planes. The asymmetry in the TD distribution is a necessity in case of the miscut substrates which is subsequently explained. In principle, the large lattice misfit between Si and GaSb is accommodated by an orthogonal network of sessile Lomer (perfect 90°) dislocations as depicted in **Figure 4a**. They are located at the interface to the substrate and relieve the epitaxial strain along the $[110]$ and $[\bar{1}\bar{1}0]$ direction. Their formation occurs during the initial 3D growth stage.^[11] In case of the miscut substrate, an additional strain component occurs parallel to the $[001]$ direction due to the lattice mismatch at the surface steps as discussed in a previous work.^[12] In order to relieve this strain component, the possible number of perfect dislocations with $\frac{a}{2}\langle 011 \rangle$ -type Burgers vectors is limited to four because a $[001]$ and a $[00\bar{1}]$ components are mutually exclusive as one increases the strain. The $[001]$ component is considered regarding the finish-start/right-hand-convention (FS/RH-convention),^[13] with the dislocation line pointing along the $[\bar{1}10]$ direction

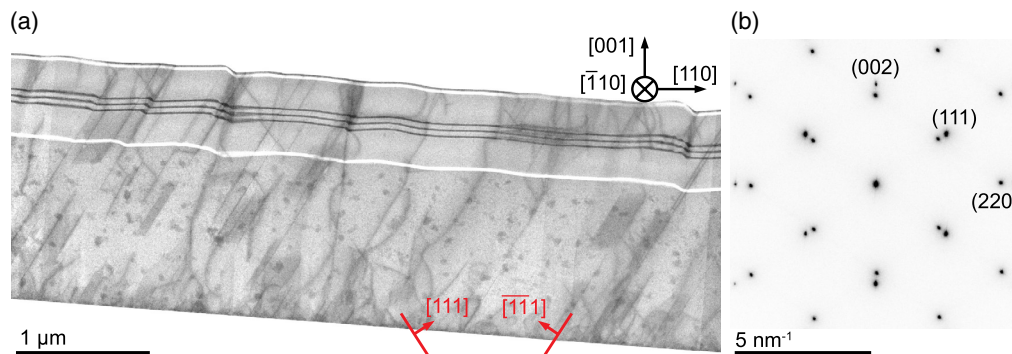


Figure 3. a) The bright-field STEM image of the cross-sectional specimen reveals a larger number of extended defects parallel to $(\bar{1}\bar{1}1)$ than to (111) lattice planes in the sample grown on a vicinal Si(001) substrate with a 7° miscut angle. b) The SAD pattern underlines the epitaxial orientation of the substrate and the buffer-layer lattices.

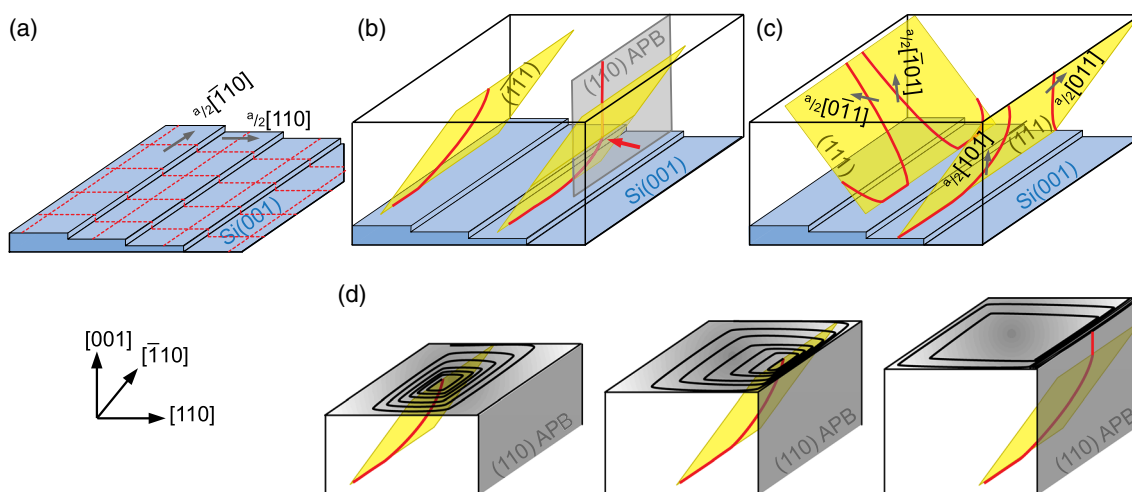


Figure 4. a) The large lattice misfit between the epitaxial GaSb buffer and the Si substrate is principally accommodated by the formation of a misfit dislocation network. The two orthogonal sets of dislocations consist of perfect 90° dislocations (dashed red lines). b) The scheme depicts the interaction of a TD (red solid line) with an APB as revealed by electron tomography investigations. c) The four considered Burgers vectors are depicted for dislocations on the (111) and $(\bar{1}\bar{1}1)$ glide planes. d) The mechanism of step bunching is illustrated regarding the evolution of a growth spiral near an APB reaching the growth front of the epitaxial layer.

and the miscut oriented as depicted in Figure 4. The line defects form 60° dislocations when gliding on {111} planes into the interface as depicted in Figure 4c. The four remaining, possible Burgers vectors (Equation (1), (2), (3), and (4)) are illustrated in 4(c). A larger number of TDs are located on ($\bar{1}\bar{1}1$) planes according to Figure 3a. This finding is explained with regard to the decomposition of Burgers vectors into the following components

$$\frac{a}{2}[101] = \frac{a}{4}[110]_{mf} + \frac{a}{2}[001]_{mf} + \frac{a}{4}[\bar{1}\bar{1}0]_{tw} \quad (1)$$

$$\frac{a}{2}[011] = \frac{a}{4}[110]_{mf} + \frac{a}{2}[001]_{mf} + \frac{a}{4}[\bar{1}\bar{1}0]_{tw} \quad (2)$$

$$\frac{a}{2}[0\bar{1}1] = \frac{a}{4}[\bar{1}\bar{1}0]_{mf} + \frac{a}{2}[001]_{mf} + \frac{a}{4}[\bar{1}\bar{1}0]_{tw} \quad (3)$$

$$\frac{a}{2}[\bar{1}01] = \frac{a}{4}[\bar{1}\bar{1}0]_{mf} + \frac{a}{2}[001]_{mf} + \frac{a}{4}[\bar{1}\bar{1}0]_{tw} \quad (4)$$

The first two components compensate for the lattice misfit (mf). Obviously, the $\frac{a}{4}[110]_{mf}$ and $\frac{a}{4}[\bar{1}\bar{1}0]_{mf}$ terms are also mutually exclusive because one relieves and the other one increases the misfit strain. The last term causes a twist (tw) between the crystal lattices. In accordance with the observations, TDs with Burgers vectors parallel to ($\bar{1}\bar{1}1$) lattice planes (Equation (1) and (2)) are more frequent. The twist components of these two dislocation types are of opposite signs. Hence, the antimonide heterostructure appears epitaxially aligned to the substrate as observed in Figure 3b.

Eventually, the following mechanism of step bunching is proposed. The prerequisites for this mechanism are a miscut substrate for epitaxial growth, an imbalanced number of TDs on symmetry-equivalent {111} lattice planes, APBs reaching the surface, and the strong interaction of the latter extended defects. Figure 4c illustrates the initial situation: A TD with a Burgers vector component and a dislocation line direction component perpendicular to the surface causes a growth spiral.^[14,15] Due to the asymmetric TD distribution, spirals exhibit a prevailing sense of rotation and they approach APBs predominantly from one side. Atomic steps floating radially from the spiral center meet the APB at the surface. It is expected that the passage of steps over the APB is energetically unfavorable as one row of like atom bonds (Sb–Sb and III–III) has to be created. Consequently, the impediment to step motion causes an accumulation of atomic steps. Finally, the TD merges into the APB and the steps pile up to form several nanometer high steps that coincide with the position of the extended defects.

It has to be mentioned that the suppression of surface steps succeeds with the avoidance of APBs reaching the surface. Respective measures have to ensure the formation of a well-established atomic double-step configuration^[16] and the removal of surface contamination^[17] by adequate treatment.^[18,19] Furthermore, the tuning of growth parameters has been shown to induce the annihilation of APBs.^[20]

In summary, several nanometer high-surface and interface steps are observed in epitaxial III–Sb layers grown on vicinal Si(001) substrates. An unexpected model of step bunching is proposed based on the interaction of TDs with APBs and an imbalanced number of dislocations on symmetry-equivalent {111} lattice planes.

Acknowledgements

The authors thank Michael Hanke for critical reading of the manuscript and acknowledge Margarita Matzeck and Astrid Pfeiffer for their support in specimen preparation and technical maintenance of the laboratories. Parts of this work have been funded by the European Union and the State of Berlin via the EFRE project 2016011843 and by the French program on “Investments for the future” (equipEX EXTRA, ANR11EQX0016).

Conflict of Interest

The authors declare no conflict of interest.

Keywords

epitaxial growth, extended defects, semiconductor heterostructures, step bunching

Received: May 20, 2019

Revised: July 2, 2019

Published online: July 26, 2019

- [1] M. Kasu, N. Kobayashi, *J. Appl. Phys.* **1995**, 78, 3026.
- [2] R. Schwoebel, E. Shipsey, *J. Appl. Phys.* **1966**, 37, 3682.
- [3] R. Schwoebel, *J. Appl. Phys.* **1968**, 40, 614.
- [4] M. Niehle, A. Trampert, J. B. Rodriguez, L. Cerutti, E. Tournié, *Scr. Mater.* **2017**, 132, 5.
- [5] J. Rodriguez, L. Cerutti, P. Grech, E. Tournié, *Appl. Phys. Lett.* **2009**, 94, 061124.
- [6] J. Reboul, L. Cerutti, J. Rodriguez, P. Grech, E. Tournié, *Appl. Phys. Lett.* **2011**, 99, 121113.
- [7] B. Galiana, I. Rey-Stolle, I. Beinik, C. Algara, C. Teichert, J. Molina-Aldareguia, P. Tejedor, *Sol. Energy Mater. Sol. Cells* **2011**, 95, 1949.
- [8] D. Chadi, *Phys. Rev. Lett.* **1987**, 59, 1691.
- [9] T. Cerba, M. Martin, J. Moeyaert, S. Avid, J. Rouviere, L. Cerutti, R. Alcotte, J. Rodriguez, M. Bawedin, H. Boutry, F. Bassani, Y. Bogumilowicz, P. Gergaud, E. Tournié, T. Baron, *Thin Solid Films* **2018**, 645, 5.
- [10] J. Taftø, J. Spence, *J. Appl. Crystallogr.* **1982**, 15, 60.
- [11] A. Rocher, E. Snoeck, *Mater. Sci. Eng. B* **1999**, B67, 62.
- [12] M. Niehle, J. B. Rodriguez, L. Cerutti, E. Tournié, A. Trampert, *Acta Mater.* **2018**, 143, 121.
- [13] The rotational direction of the Burgers circuit around the dislocation line is defined by the fingers of the right hand (RH). The thumb points along the dislocation line. The Burgers vector is directed from the finish to the start point (FS).
- [14] H. Strunk, *J. Cryst. Growth* **1996**, 160, 184.
- [15] D. Woodruff, *Philos. Trans. R. Soc., A* **2015**, 373, 20140230.
- [16] D. Aspnes, J. Ihm, *Phys. Rev. Lett.* **1986**, 57, 3054.
- [17] C. Barrett, A. Lind, X. Bao, Z. Ye, K. Ban, P. Martin, E. Sanchez, Y. Xin, K. Jones, *J. Mater. Sci.* **2016**, 51, 449.
- [18] K. Madiomanana, M. Bahri, J. Rodriguez, L. Largeau, L. Cerutti, O. Mauguin, A. Castellano, G. Patriarche, E. Tournié, *J. Cryst. Growth* **2015**, 413, 17.
- [19] B. Kunert, I. Nemeth, S. Reinhard, K. Volz, W. Stolz, *Thin Solid Films* **2008**, 517, 140.
- [20] I. Németh, B. Kunert, W. Stolz, K. Volz, *J. Cryst. Growth* **2008**, 310, 1595.